Preprints of the 19th World Congress
The International Federation of Automatic Control
Cape Town, South Africa. August 24-29, 2014

Development of a Wheel-Type Robot Tractor and its Utilization

Liangliang YANG, Noboru NOGUCHI*

Vehicle Robotics Laboratory, Graduate School of Agriculture, Hokkaido University, Kita-9, Nishi-9, Kita-ku, Sapporo, 060-8589, Japan; (e-mail: yang@bpe.agr.hokudai.ac.jp, noguchi@ bpe.agr.hokudai.ac.jp)

Abstract: This article described the development and utilization of a CAN-bus based robot tractor. A RTK-GPS and an IMU were utilized as a position and a posture sensor for the development of a navigation system. The path planning and navigation control method were described in this article. Three field tests were conducted to show the performance and stability of the robot on straight path, logged path following crop rows and long time work. The RMS value of lateral and heading errors of three tests were 0.05 m and 0.6 degree, 0.02 m and 0.77 degree, 0.04 m and 0.75 degree, respectively. The results revealed the CAN-bus based robot tractor has high and stable navigation accuracy. The accuracy was acceptable for all tests.

1. INTRODUCTION

Robot tractor is a key technology to solve the problem of descending number and aging of farmers. The positioning system for a robot tractor has been developed using a machine vision early from 1980's in a field by detecting out a directrix from crop rows (Reid and Searcy, 1988; Billingsley and Schoenfisch, 1995). And, some augmented algorithms were proposed to improve the ability of the crop row detection (Olsen, 1995; Hague and Tillett, 2001). In our laboratory, a stereo camera has been adopted to detect the navigation directrix (Kise et al., 2005). In addition, a laser scanner was selected as a positioning sensor in an orchard (Barawid et al., 2007). However, the lack of reference objects could result in a failed to determine the position. A reference objects independent positioning system was available in 1990's when U.S. department of defense created a Global Positioning System (GPS). The GPS was utilized for a tractor (Stombaugh et al., 1998; Kise et al., 2000) and a rice transplanter (Nagasaka et al., 2004). And, high navigation accuracy could be obtained using a real time kinematic GPS (RTK-GPS). Therefore, in this study a RTK-GPS receiver was used as a position sensor.

However, from the experiences of our laboratory, modifications of a tractor must be conducted so that a manual tractor could be modified to a robot tractor for those prior researches. Today, controller area network bus (CAN-bus) based tractor enable developers can control the vehicle by an electronic control unit (ECU) of the tractor easier than ever before. Moreover, a structure of a controller for a robot tractor could be shifted from one tractor to the other very easily in case both were based on CAN-bus. This can reduce the cost for using robot tractors.

This study aimed to develop a new robot tractor using a commercial wheel-type CAN-bus based tractor. The CAN-bus for implement was followed the ISOBUS (ISO 11783) protocol. The RTK-GPS was selected as a navigation sensor. An omni-directional safety system and an emergency stop system were also installed on the robot tractor in order to improve its safety. In this study, three tests were conducted to show the performance of the developed robot tractor.

2. TRACTOR PLATFORM AND NAVIGATION SENSORS

2.1 Tractor platform

In this study, a wheel type tractor (EG83, YANMAR Co., Ltd., Japan) was utilized as a tractor platform to develop a robot tractor. The specifications of the tractor are engine power of 61 kW, height, width and length of 2.620, 1.750 and 3.905 m, respectively, and mass of 2840 kg. The control units of the tractor system are shown in Fig. 1, which include an engine controller, a Hydraulic Mechanical Transmission (HMT) controller, a Hitch controller, a Tractor ECU (TECU), meters and a control PC for the robot tractor.

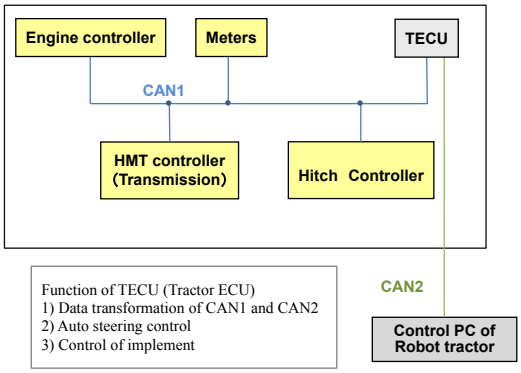

Fig. 1. The control units of the tractor.

The engine controller is used to control the rotation speed of the engine and the HMT controller is used to control the transmission in order to control the vehicle speed. The hitch controller is used to control the height of implement. The meters are used to measure and to show the vehicle status, such as engine rotation speed, vehicle speed, hitch position, PTO rotation speed, etc. The TECU was applied to transform the data between CAN1 and CAN2, control the hydraulic power auto steering unit as well as the implement.

The control PC of the robot tractor is using Windows® operation system (OS) that is used to perform all the jobs of robot control, such as path-planning, calculating steering angle, parsing command code, transmitting control parameters to the tractor and receiving feedback information from the tractor. And only this control PC is installed to the tractor by us, the other controllers and meters are totally embedded to the tractor already for commercial market.

The schematic diagram of the robot tractor system is shown on a picture of the robot tractor of this study in Fig. 2. A control PC is installed to the tractor in order to fulfil the robot control function; and the other PC for a safety system is used to obtain information from an omni-directional stereo vision (OSV), a front and a rear laser scanner to detect obstacles near the tractor. The detail of the safety system could be read from published papers (Yang and Noguchi, 2012, Yang, 2013).

As shown in Fig. 1 and Fig. 2, there are two CAN-bus in this robot tractor system. CAN1 is a CAN-bus that was utilized to transform the information in side of the tractor, while CAN2 is a CAN-bus followed ISOBUS protocol that was adopted as an implement BUS in order to communicate between the control PC of the robot tractor, the PC of the safety system, implement and TECU.

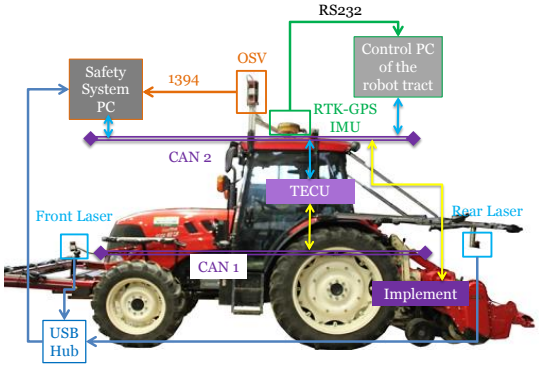

Fig. 2. Schematic diagram of the robot tractor system.

2.2 Navigation Sensors

The navigation sensor is an RTK-GPS receiver (AGI3, Topcon Co., Ltd., Japan) integrated an Inertial measurement unit (IMU) as illustrated in Fig. 3. The horizontal position accuracy of the RTK-GPS is around ±0.03 m.

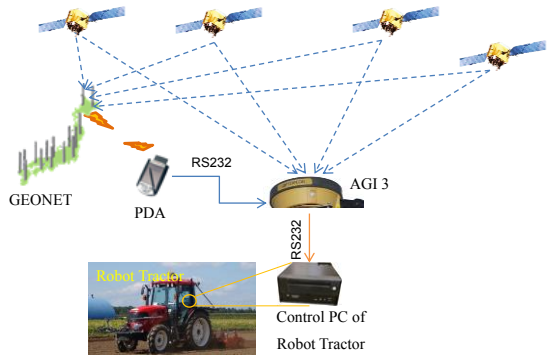

Fig. 3. Schematic diagram of the RTK-GPS system.

In Fig. 3, A PDA connected to internet via a 3G mobile phone network is used to acquire the correctional signal from a GPS Earth Observation Network (GEONET) service of Japan. And the correctional signal is transmitted to the RTK-GPS receiver (AGI 3) via a RS232 cable. The drift error of heading angle of the IMU is corrected by the RTK-GPS. The position and the posture data are sent to the control PC of the robot tractor by a RS232 at 10 Hz.

3. NAVIGATION METHOD

A pre-planned navigation map is necessary before letting a robot tractor to run in a field. In this study, the navigation map is defined with two functions: one is to decide working paths for the robot; the other is to decide working condition of implement on all points of the map. The working condition was defined by a code that includes the engine speed, vehicle speed, PTO (on/off), hitch (up/down). In a rectangular field, firstly, a manually survey of four corners position of a working field is necessary to define a working space. Secondly, the space is segmented into paths according to the implements width and the field width. Fig. 4 shows a navigation map example. The navigation path is defined by the latitude and longitude of all points in the world coordinates. The third dimension defines the working command that was encoded according to a pre-defined format. A data set example (43.0744415, 141.336513, 115459) corresponding to the last point (red colour) of path 1 is shown in Fig. 4.

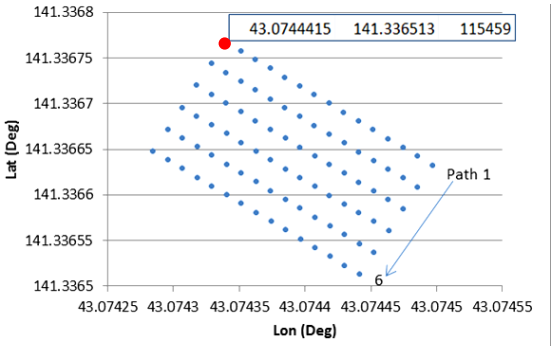

Fig. 4. A navigation map.

Fig. 5 illustrates a block diagram of control flow for the robot tractor in this study. At first, the navigation map is read by a navigator; and the position, velocity and posture data are obtained from the RTK-GPS and the IMU, and transmitted to the navigator at the same time.

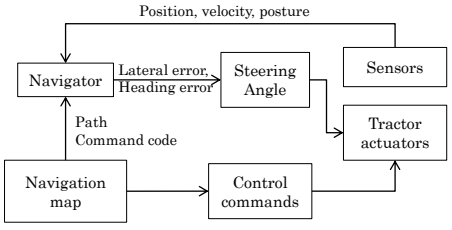

Fig. 5. Block diagram of control flow for the robot tractor.

At second, the steering angle ($\Delta\psi$) was calculated based on a lateral error and a heading error bearing from the pre-created path by Eq. (1). In addition, control commands for the implement, such as PTO (on/off), hitch (up/down), were decoded from the codes embedded in the navigation map.

$$\Delta\psi = -(k_\varphi \Delta\varphi + k_d d) \tag{1}$$

where, d is the lateral error; $\Delta\varphi$ is the heading error; k_φ and k_d are decided by experiment. In this study, they are 1.5 and 20, respectively.

The lateral error, d, was the shortest distance from the current position of the tractor measured by the RTK-GPS to the path.

The heading error, $\Delta\varphi$, was calculated from the relative angle between the desired angle and actual heading angle in the ground coordinates, where the desired angle was defined by the vector that was spanned by the orthogonal projection of current robot position on the map trail and the other point that distance to the projection with a look ahead distance, which was set as 5m in this study; while the actual heading was measured by the IMU.

At last, the steering angle and the control commands were sent to the TECU by the CAN2 as shown in Fig. 1 in order to control the actuators of the tractor.

There is a position data error introduced by inclinations of the tractor. In order to reduce this error, the position data from the RTK-GPS is corrected by using the posture data by Eq. (2):

$$\mathbf{P}' = \mathbf{P} - \mathbf{E} \bullet \mathbf{A} \tag{2}$$

$$\mathbf{P}' = [x', y', z']^T$$

$$\mathbf{P} = [x, y, z]^T$$

$$\mathbf{A} = [a, b, h]^T$$

$$\mathbf{E} = \begin{bmatrix} \cos\theta_r \cos\phi + \sin\theta_r \sin\theta_p \sin\phi & \cos\theta_p \sin\phi & -\cos\theta_r \sin\theta_p \sin\phi + \sin\theta_r \cos\phi \\ -\cos\theta_r \sin\phi + \sin\theta_r \sin\theta_p \cos\phi & \cos\theta_p \cos\phi & -\cos\theta_r \sin\theta_p \cos\phi - \sin\theta_r \sin\phi \\ -\sin\theta_r \cos\theta_p & \sin\theta_p & \cos\theta_r \cos\theta_p \end{bmatrix}$$

where, $\mathbf{P}'$ is the corrected position data; $\mathbf{P}$ is the raw position data from the RTK-GPS; a and b are the offset of the RTK-GPS antenna from the centre of form (COF) along longitudinal, lateral direction of the tractor; and h is the height of the antenna from the surface of ground in vertical direction; θ_r, θ_p and ϕ are the roll, pitch and heading angle of the tractor measured by the IMU.

The field size is small in Japan. And, farmers are always turning their tractors on the road near to their field. In this study we are trying to follow this culture. And the path for headland turning was not pre-created. A switch-back turning pattern was designed to navigate the tractor turning from one path to the other path. More details of the turning method could be read from the articles of our laboratory (Kise et al., 2002; Yang, 2013).

4. FIELD TEST RESULTS AND DISCUSSIONS

In order to show the performance of the developed robot tractor system, three field tests for different utilizations were conducted at different places of Hokkaido, Japan.

4.1 Test one – navigation without implement

The first test was conducted at an experiment farm for test the navigation accuracy without implement in Hokkaido University, Sapporo, Hokkaido, Japan. It is conducted to evaluate the accuracy of the navigation system for straight paths. The vehicle speed was 1.0 m/s. The navigation map and a trajectory of the robot tractor are shown in Fig. 6. It can be seen that the robot trajectory was exactly covered the map.

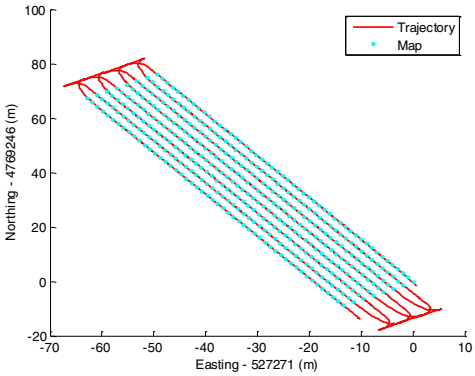

Fig. 6. Navigation map and trajectory of the robot tractor of the first test. (Easting and northing are shifted 527271 m and 4769246 m in UTM coordinates in order easier show the size of the map)

The lateral and heading error of all the 8 paths on the working area (not including turning area where does not have navigation map to calculate lateral and heading error) of the test are shown in Fig. 7(a) and Fig. 8(a), respectively.

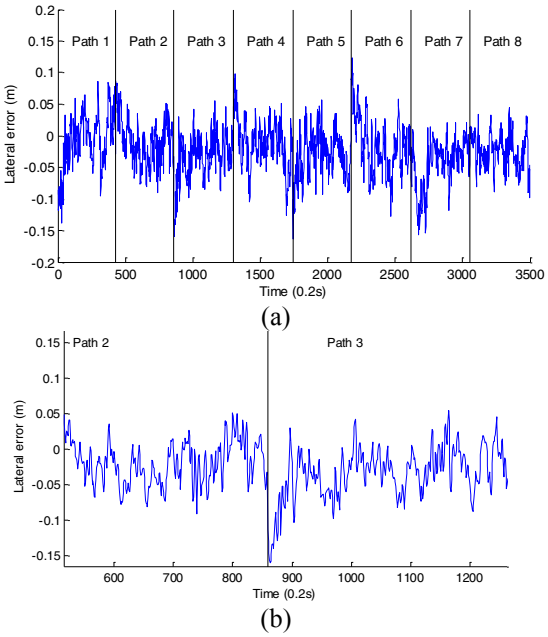

Fig. 7. Lateral error of the first test. (a) Lateral error of all paths; (b) Zoom-in area of Lateral error of Path 2 and Path 3.

From these two figures, it can be seen that both lateral and heading errors were varying around zero. However, the lateral error was a little high after turning. Fig. 7(b) shows a zoom-in area of path 2 and path 3 of lateral error. The lateral error decreased from a high error (-0.15 m) to a low error (-0.08 m) costing about 2 s. In addition, Fig. 8(b) shows an zoom-in area of path 2 and path 3 of the heading error. The heading error was already lowered to a stable level (around ±1.5°) after turning. The average value of the maximum, minimum and RMS of lateral error of the 8 paths were 0.07, -0.13 and 0.05 m, respectively. And the average of maximum, minimum and RMS of heading error in the 8 paths are 1.58, -1.15 and 0.57 degree, respectively. From this result, it can be seen that the developed robot tractor can automatically run at an accuracy of around 0.05 m and 0.6 degree for lateral error and heading error, respectively, on straight paths. This accuracy was high enough for auto navigation of a robot tractor in a field.

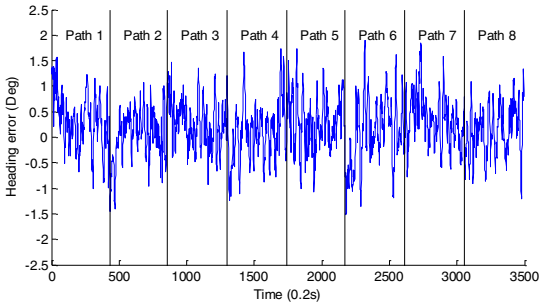

(a)

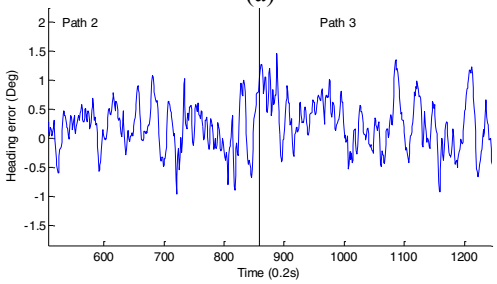

(b)

Fig. 8 Heading error of the first test. (a) Heading error of all paths; (b) Heading error of the connection area of Path 2 and Path 3.

4.2 Test two – navigation along crop rows

The second test was carried out at a soybean field at an experiment farm of Hokkaido University for spraying in order to test the navigation flexibility when running on a non-straight navigation path. The path was logged when human driving along crop rows using RTK-GPS, so that the robot tractor could be navigated following the crop rows without rolled over them.

Fig. 9 illustrates a picture of the spraying test condition. Fig. 10 illustrates the navigation map and trajectory of the robot tractor. From Fig. 10, it can be seen that the robot tractor could following the pre-logged path correctly.

Fig. 9 The spraying test condition.

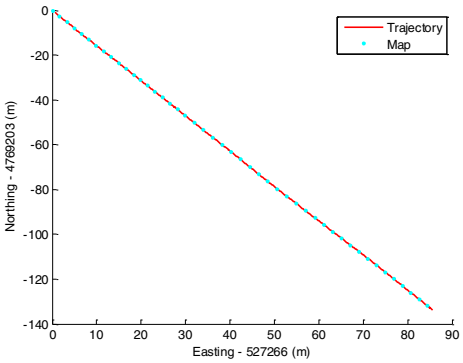

Fig. 10. Navigation path and trajectory of the robot tractor of the second test. (Easting and northing are shifted 527266 m and 4769203 m in UTM coordinates)

Fig. 11 and Fig. 12 show the lateral error and heading error of the spraying test, from which it can be seen that the lateral and heading errors are similar with the first test. The average value of the maximum, minimum and RMS of lateral errors were 0.03, -0.07, 0.02 m, respectively. And the average of maximum, minimum and RMS of heading errors are 1.93, -1.83, 0.77 degree, respectively.

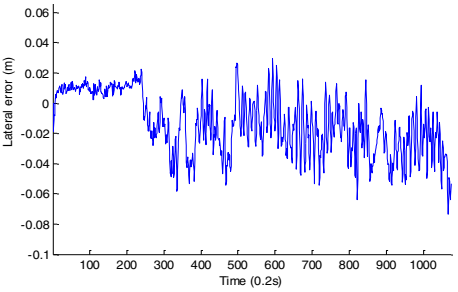

Fig. 11. Lateral error of the spraying test.

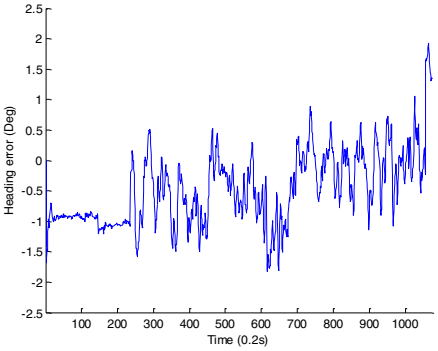

Fig. 12. Heading error of the spraying test.

The reason of the accuracy is a little lower than the first test is considered that the steering becomes heavier because of the weight of the spray tank. The navigation accuracy is enough for spraying without rolled over crops in the test condition. And at the ending points (after data sampling about 1000) of Fig. 11 and Fig. 12, there is a drop of accuracy for both lateral error and heading error. The reason for the drop of accuracy is that at the end of the path the front tyre went to road in the test. And there was a step between the soybean field and road. At that time, the robot tractor has already finished job for one path, therefore we do not need to care for this drop of accuracy. In the fact, headland turning on a road in front of a field is normal in Japan because the field size is small and the farmers always don't want to run repeatedly on a same field in order to reduce pressure to the field.

4.2 Test three – navigation at night for long-time tillage

The third test was conducted at night for long-time tillage utilization a field of Hokuto Yanmar Co., Ltd., Ebetsu, Hokkaido, Japan. The field size for tillage was about 2 ha. The test was started around 5:20 PM and finished at 10:05 PM (4 hours 45 minutes) in order to test the stability of the navigation system for long-time work. There was not any operation of human to the robot tractor when it was working.

The coverage width of a path was 2.2 m, and the length was about 200 m. The field width was around 100 m. Total number of paths was 44. The working path order was from 1 to 44 in increasing order. The vehicle speed was 0.6 m/s at working. The navigation map and the trajectory of robot tractor are shown in Fig. 13. It can be seen that the trajectory was exactly covered the navigation map.

Fig. 13 The navigation map (blue) and running trajectory (red) of the robot tractor of the long-time tillage test.

The lateral and heading errors of the second test in the working area are illustrated in Fig. 14 and Fig. 15, respectively. Both errors were stable in the total 4 hours and 45 minutes test. The average values of the maximum, minimum and RMS of the lateral error over 44 paths were 0.10, -0.14 and 0.04 m, respectively. And the average values of the maximum, minimum and RMS of the heading error of all 44 paths are 2.39, -2.51 and 0.75 degree, respectively. These results reflected a same accuracy with the first test. This accuracy was stable and precise enough for an auto navigation of a robot tractor for tillage at night.

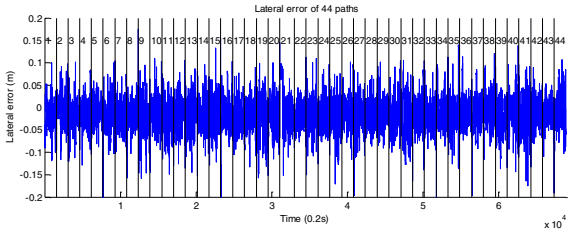

Fig. 14 The lateral error of the long-time tillage test.

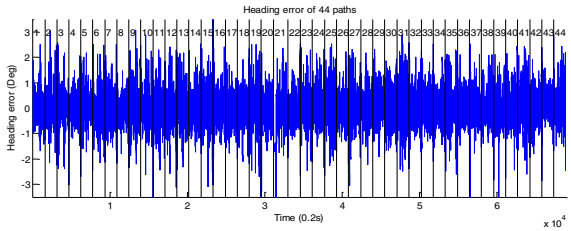

Fig. 15 The heading error of the long-time tillage test.

5. CONCLUSIONS

A CAN-bus based robot tractor was developed in this study. A task planning method was introduced to define a navigation map to decide the working space and control parameters of the robot tractor. The steering angle was calculated based on a lateral error and heading error. Three tests for different utilizations were conducted at three fields in order to evaluate the stability and accuracy of the robot tractor. The first test results indicated that the RMS of lateral and heading errors on straight paths were around 0.05 m and 0.6 degree, respectively. The second test results revealed that the robot tractor could follow a pre-logged path with the RMS value of 0.02 m and 0.77 degree of lateral and heading errors for spraying. The third test results revealed that the robot tractor could work for a long-time (4 hours and 45 minutes) for tillage with a stable accuracy. The lateral and heading error were around 0.04 m and 0.75 degree, respectively. It was concluded that the developed CAN-bus based robot tractor had stable and high navigation accuracy. The accuracy was acceptable for a robot tractor working in a real field for tillage and spraying.

REFERENCES

Barawid, J.O.C., Mizushima, A., Ishii, K., Noguchi, N., 2007. Development of an Autonomous Navigation System using a Two-dimensional Laser Scanner in an Orchard Application. Biosystems Engineering (96), 139-149.

Billingsley, J., Schoenfisch, M., 1995. Vision-guidance of agricultural vehicles. Autonomous Robots (2), 65-76.

Hague, T., Tillett, N.D., 2001. A bandpass filter-based approach to crop row location and tracking. Mechatronics (11), 1-12.

Kise, M., Noguchi, N., Ishii, K., Terao, H., 2000. Development of of the agricultural autonomous tractor with DGPS. Japanese society of agricultural machinery (62), 145-153.

Kise, M., Noguchi, N., Ishii, K., Terao, H. Enhancement of turning accuracy by path planning for robot tractor. Automation Technology for Off-Road Equipment, Proceedings of the July 26-27, 2002 (Chicago, Illinois, USA), 398-404.

Kise, M., Zhang, Q., Rovira Más, F., 2005. A Stereovision-based Crop Row Detection Method for Tractor-automated Guidance. Biosystems Engineering (90), 357-367.

Nagasaka, Y., Umeda, N., Kanetai, Y., Taniwaki, K., Sasaki, Y., 2004. Autonomous guidance for rice transplanting using global positioning and gyroscopes. Computers and Electronics in Agriculture (43), 223-234.

Olsen, H.J., 1995. Determination of row position in small-grain crops by analysis of video images. Computers and Electronics in Agriculture (12), 147-162.

Reid, J.F., Searcy, S.W., 1988. An Algorithm for Separating Guidance Information from Row Crop Images. Transactions of the ASAE (31), 1624-1632.

Stombaugh, T., E., B., Hummel, J.W., 1998. Automatic guidance of agricultural vehicles at high field speeds, ASAE paper 983110, St. Joseph. MI.

TeeJet Technologies, 2007. An Introduction to ISOBUS and Its Importance to You. A Catalog of TeeJet Technologies, Inc.

Yang, L. 2013. Development of a Robot Tractor Implemented an Omni-directional Safety System. Ph.D. diss., Graduate School of Agriculture, Hokkaido University, Sapporo.

Yang, L., Noguchi, N., 2012. Human detection for a robot tractor using omni-directional stereo vision. Computers and Electronics in Agriculture (89), 116-125.